Supplement of Atmos. Chem. Phys., 24, 12143–12160, 2024
https://doi.org/10.5194/acp-24-12143-2024-supplement

Atmospheric Chemistry and Physics
Open Access

Supplement of

Source apportionment of particle number size distribution at the street canyon and urban background sites

Sami D. Harni et al.

Correspondence to: Sami D. Harni (sami.harni@fmi.fi)

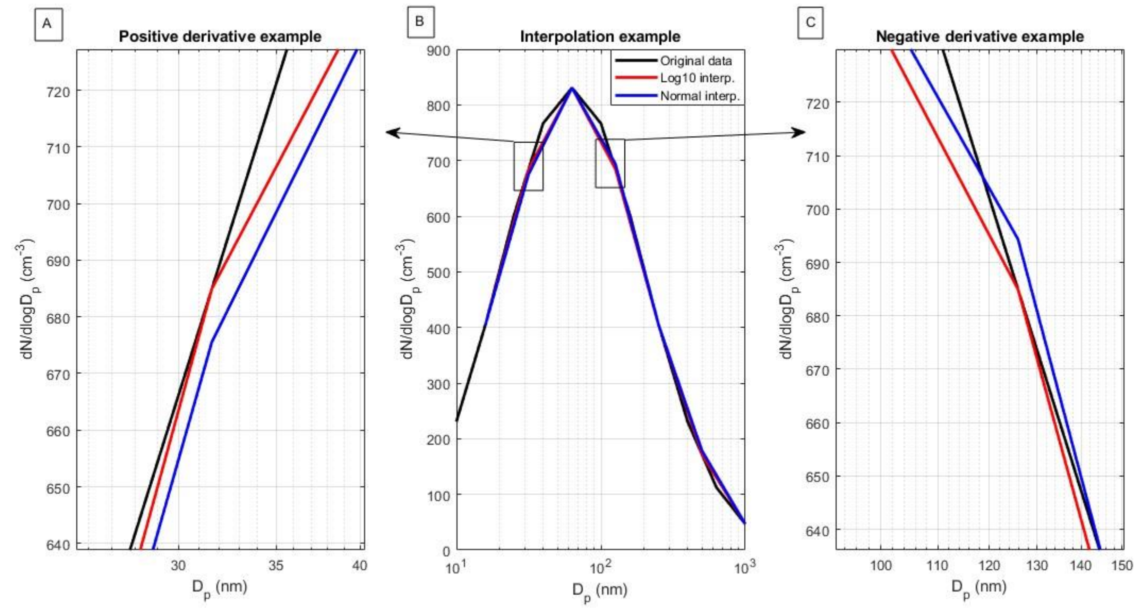

Figure S1: The figure illustrates the inaccuracies in the concentration when interpolating NSD without the logarithmic y-axis. Specially, it shows how concentrations can be underestimated when the derivative of the NSD curve is positive (Panel A), and overestimated when the derivative is negative (Panel C). Panel B provides a view of the entire NSD curve.

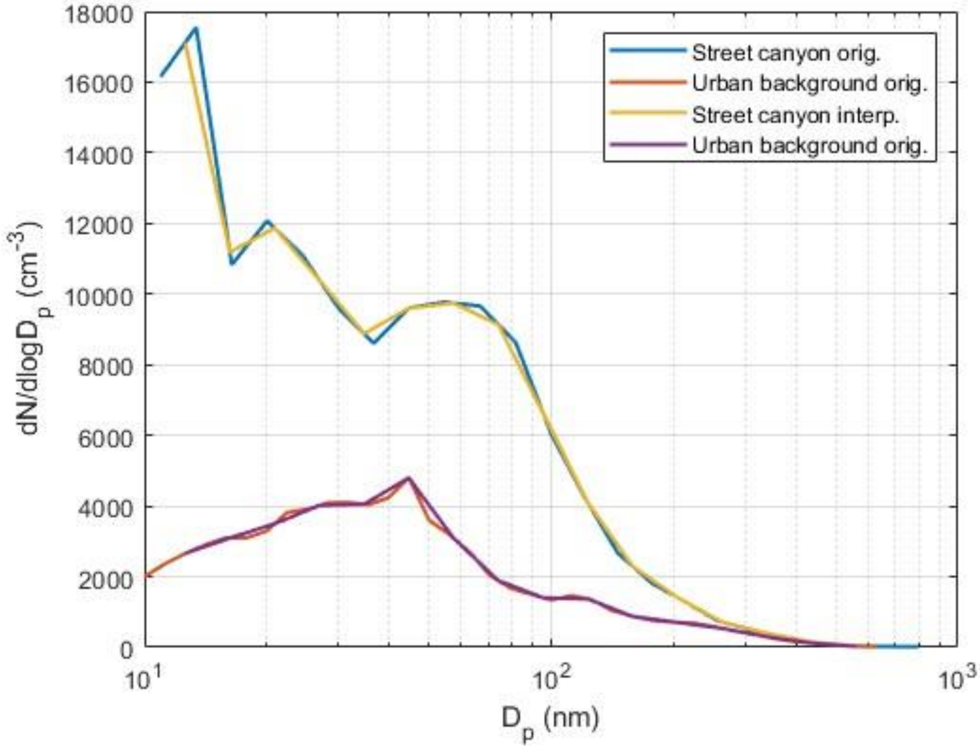

Figure S2: Example of 1 h average data the original data compared to the interpolated data for Street Canyon and Urban background sites.

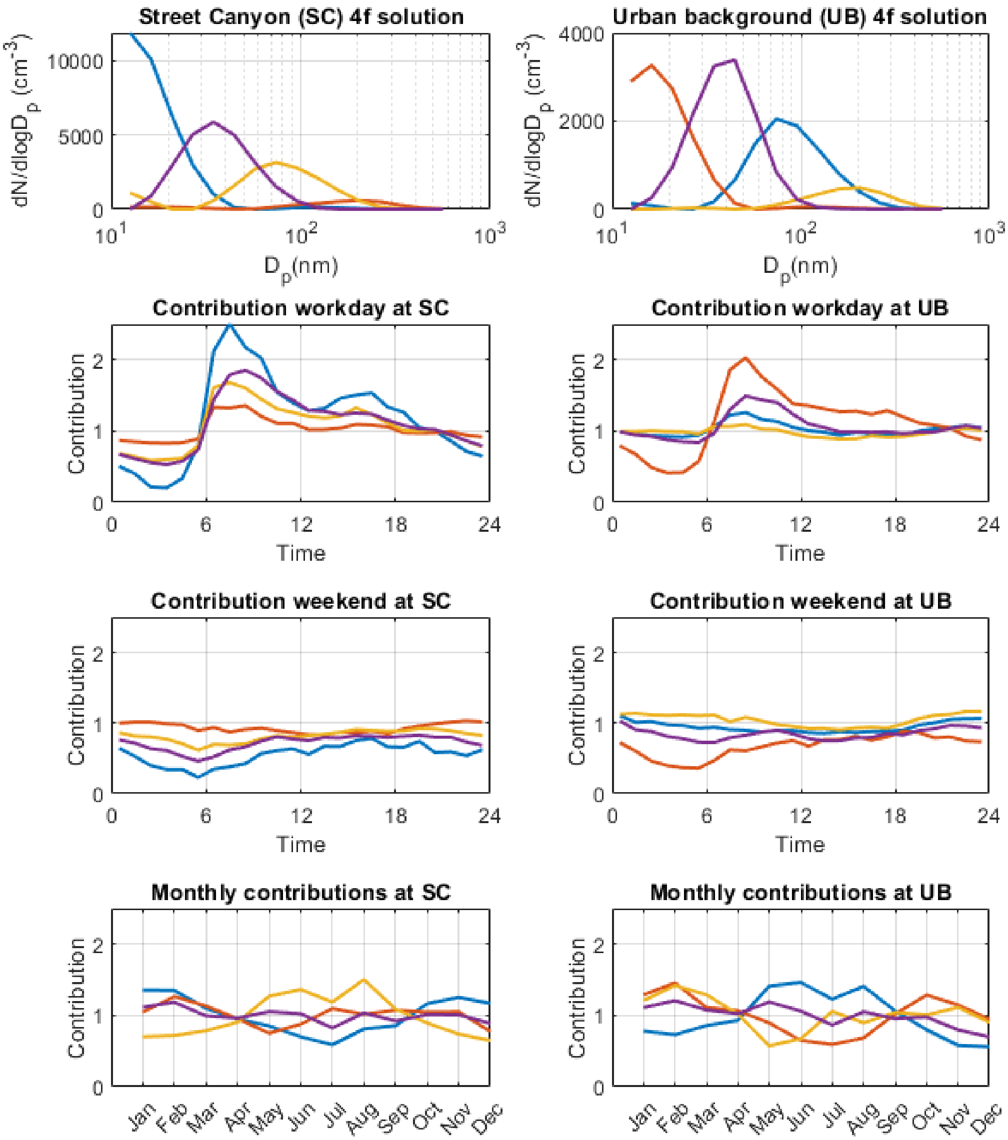

10

Figure S3: Four-factor solutions, contributions during workdays, weekends, and different months from PMF analyses done separately for SC (left column) and UB (right column).

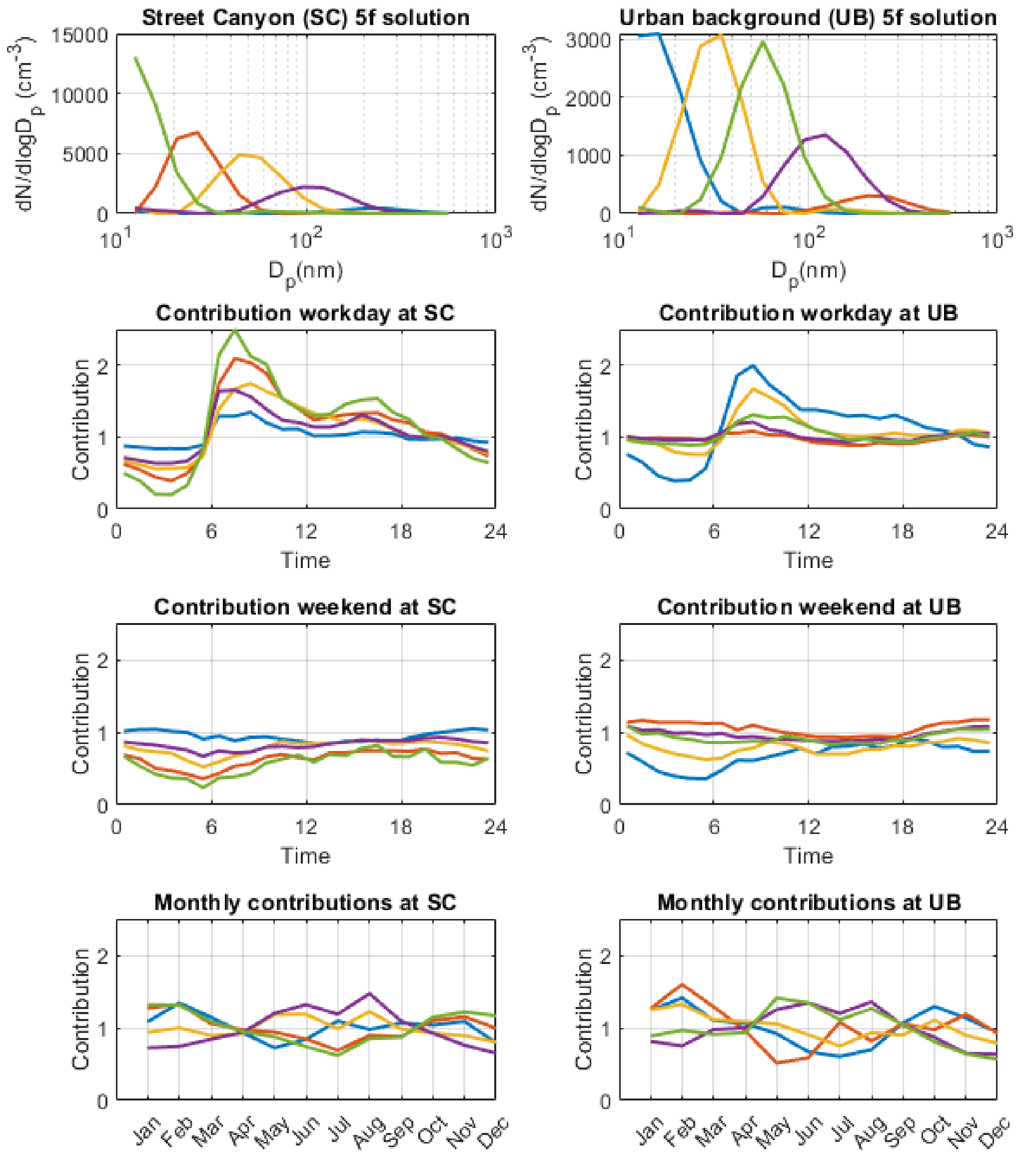

15 **Figure 4S: Five-factor solutions, contributions during workdays, weekends, and different months from PMF analyses done separately for SC (left column) and UB (right column).**

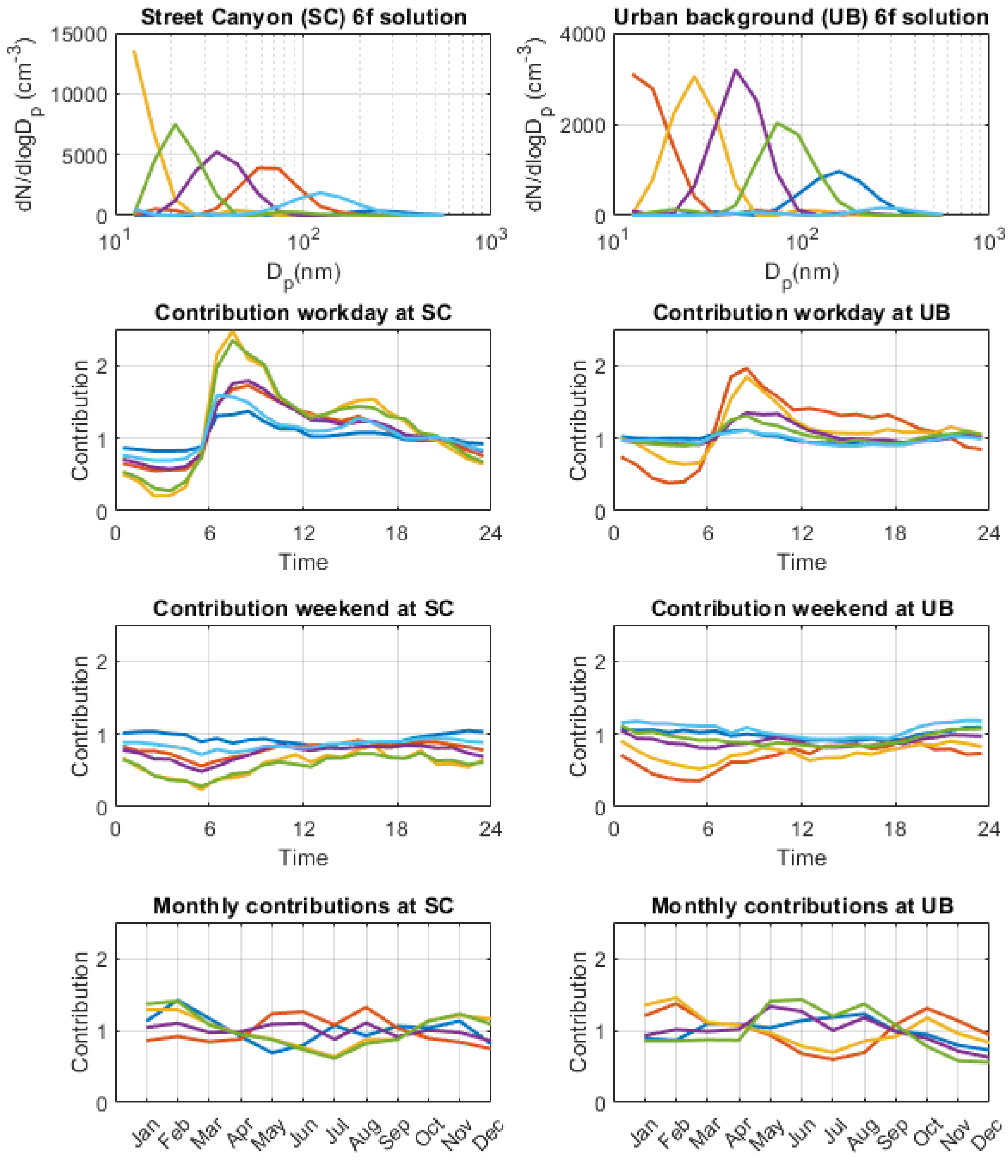

Figure S5: Six-factor solutions, contributions during workdays, weekends, and different months from PMF analyses done separately for SC (left column) and UB (right column).

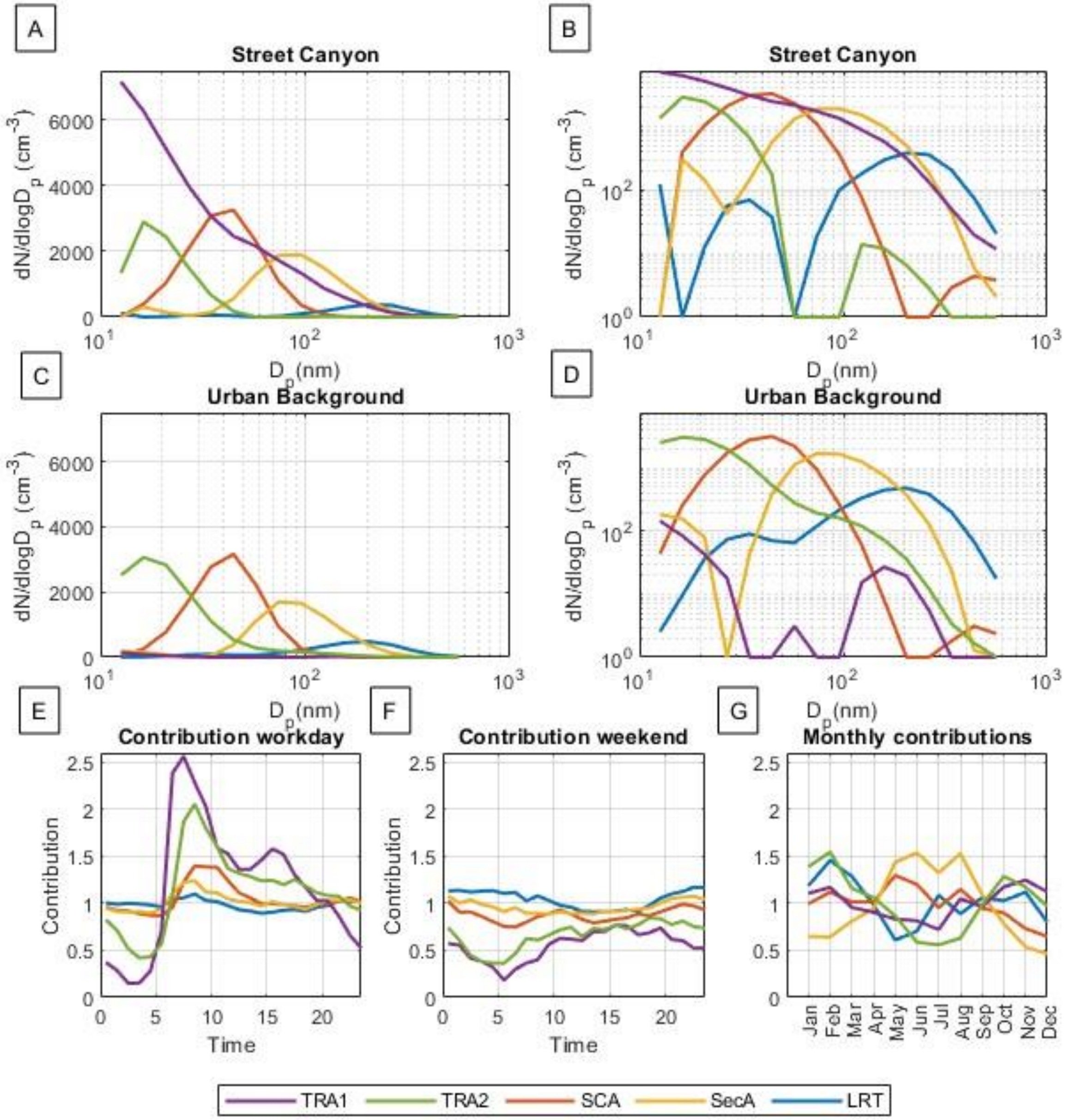

20 **Figure S6: Dispersion normalized five-factor solution of positive matrix factorization (PMF) factors presented for both stations on linear (A for SC, C for UB) and logarithmic x-axis. E presents the hourly relative contributions during workdays, F during weekends, and G the average monthly contributions. Note that the linear scale for plots A and B is different. The value presented in contribution figures is the factor with which to multiply the factor profile at any current time to get the total contribution. The average for the contribution factor is 1 over the whole measurement period for all the factors.**

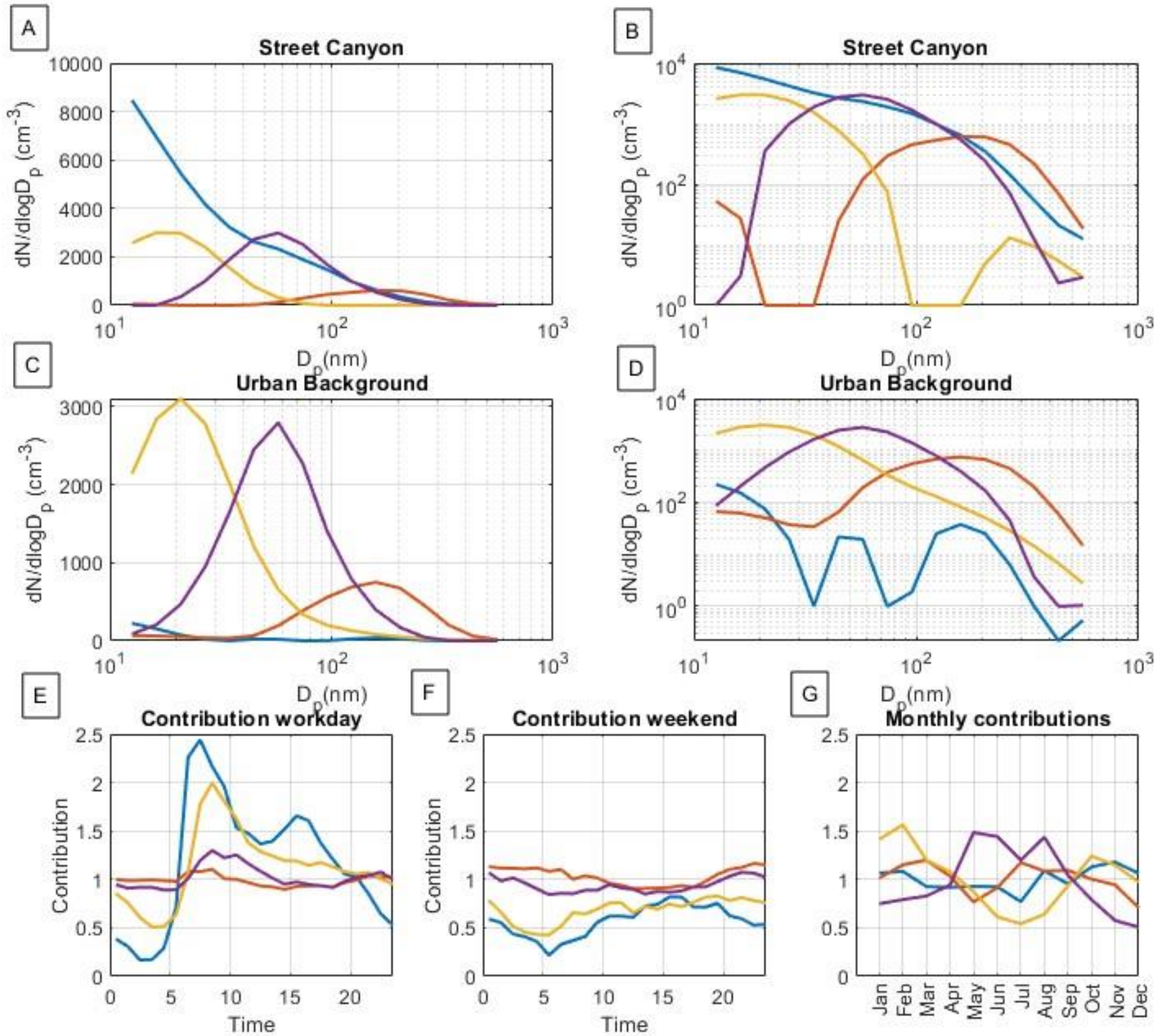

Figure S7: Four-factor solution of positive matrix factorization (PMF) factors presented for both stations on linear (A for SC, C for UB) and logarithmic x-axis. E presents the hourly relative contributions during workdays, F during weekends, and G the average monthly contributions. Note that the linear scale for plots A and B is different. The value presented in contribution figures is the factor with which to multiply the factor profile at any current time to get the total contribution. The average for the contribution factor is 1 over the whole measurement period for all the factors.

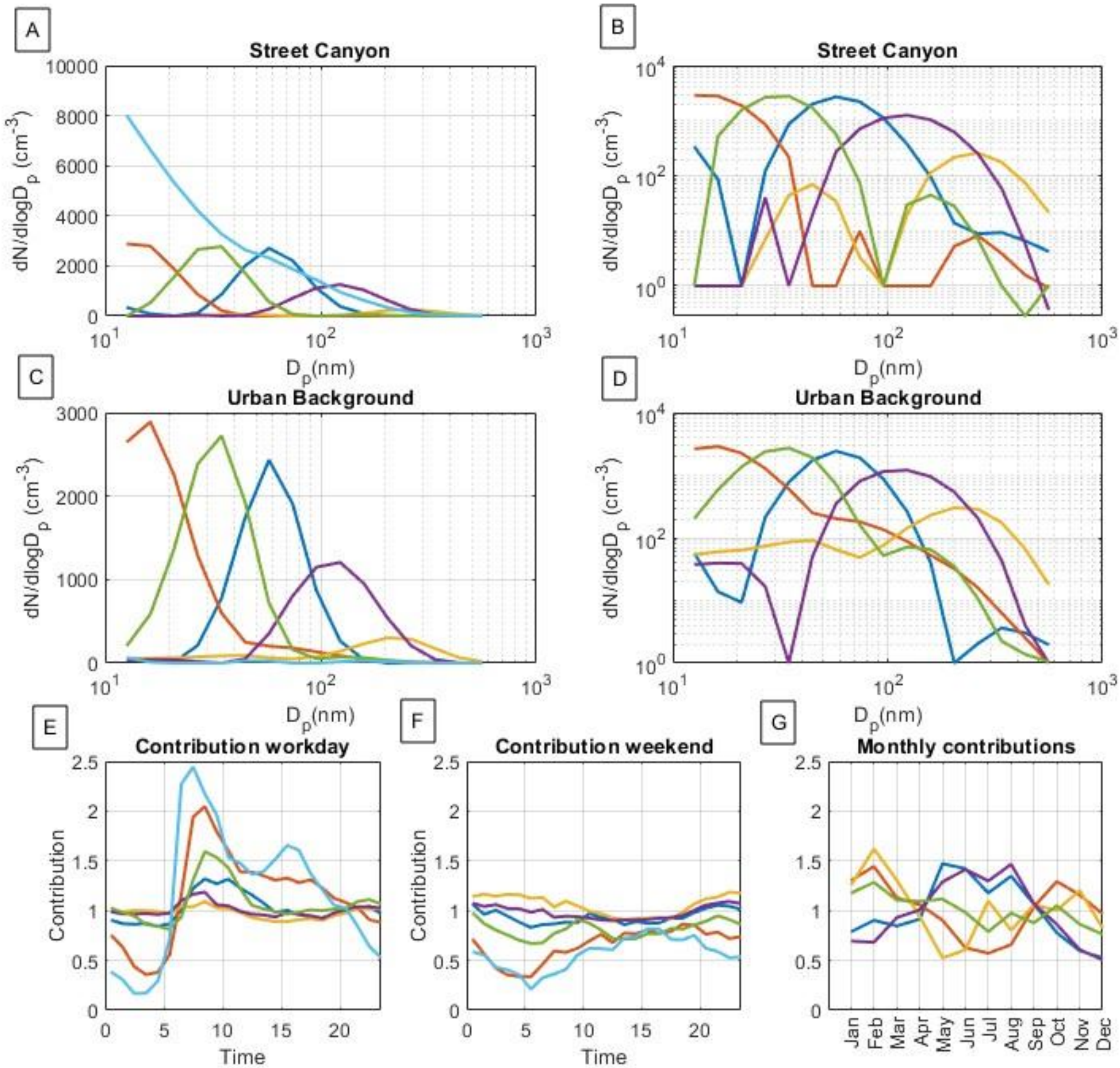

Figure S8: Six-factor solution of positive matrix factorization (PMF) factors presented for both stations on linear (A for SC, C for UB) and logarithmic x-axis. E presents the hourly relative contributions during workdays, F during weekends, and G the average monthly contributions. Note that the linear scale for plots A and B is different. The value presented in contribution figures is the factor with which to multiply the factor profile at any current time to get the total contribution. The average for the contribution factor is 1 over the whole measurement period for all the factors.

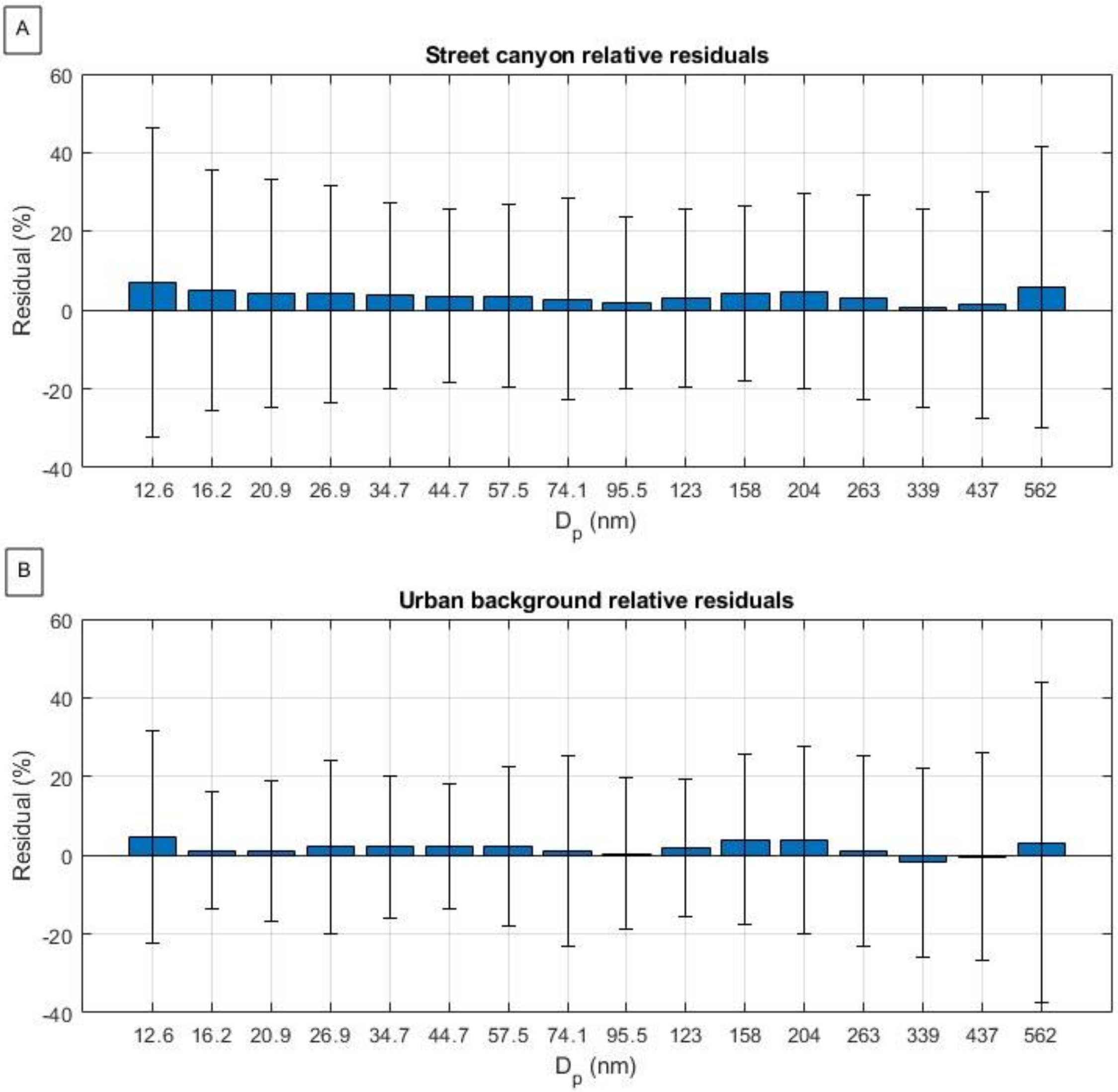

Figure S9: Relative residuals with standard deviations presented for each size bin at SC (A) and UB (B) sites.

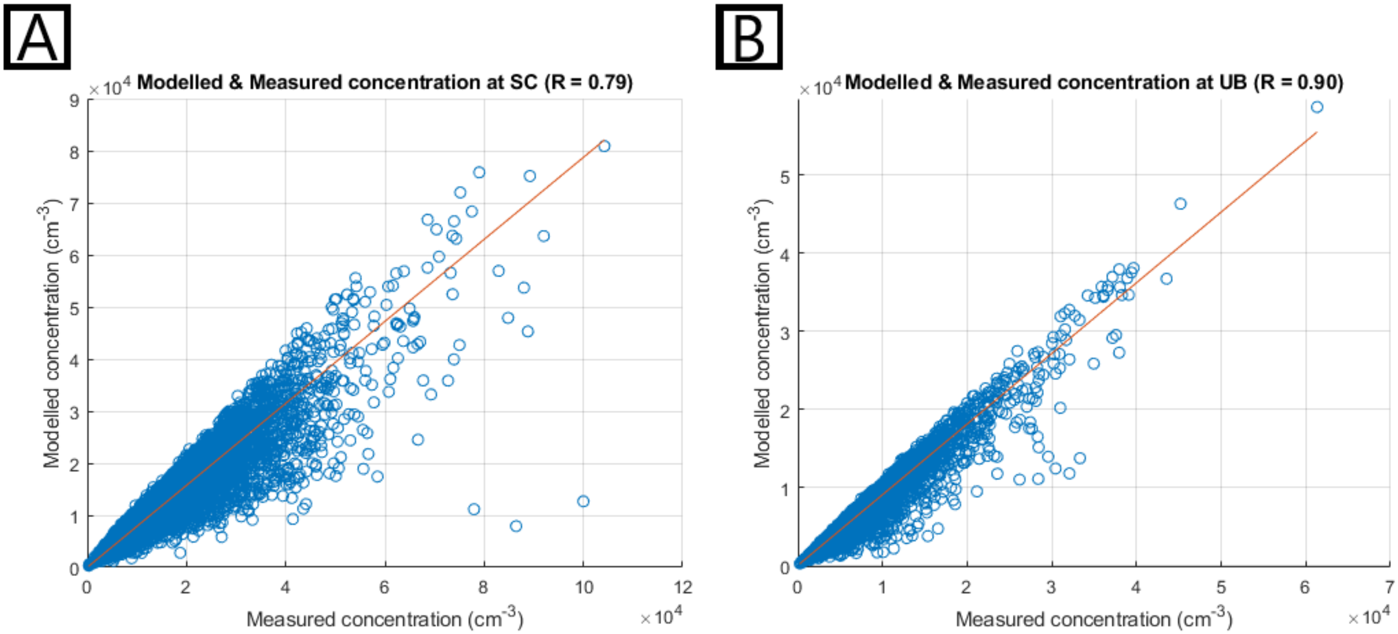

Figure S10: Regression plots between modelled and measured interpolated concentrations at SC (A) and UB (B).

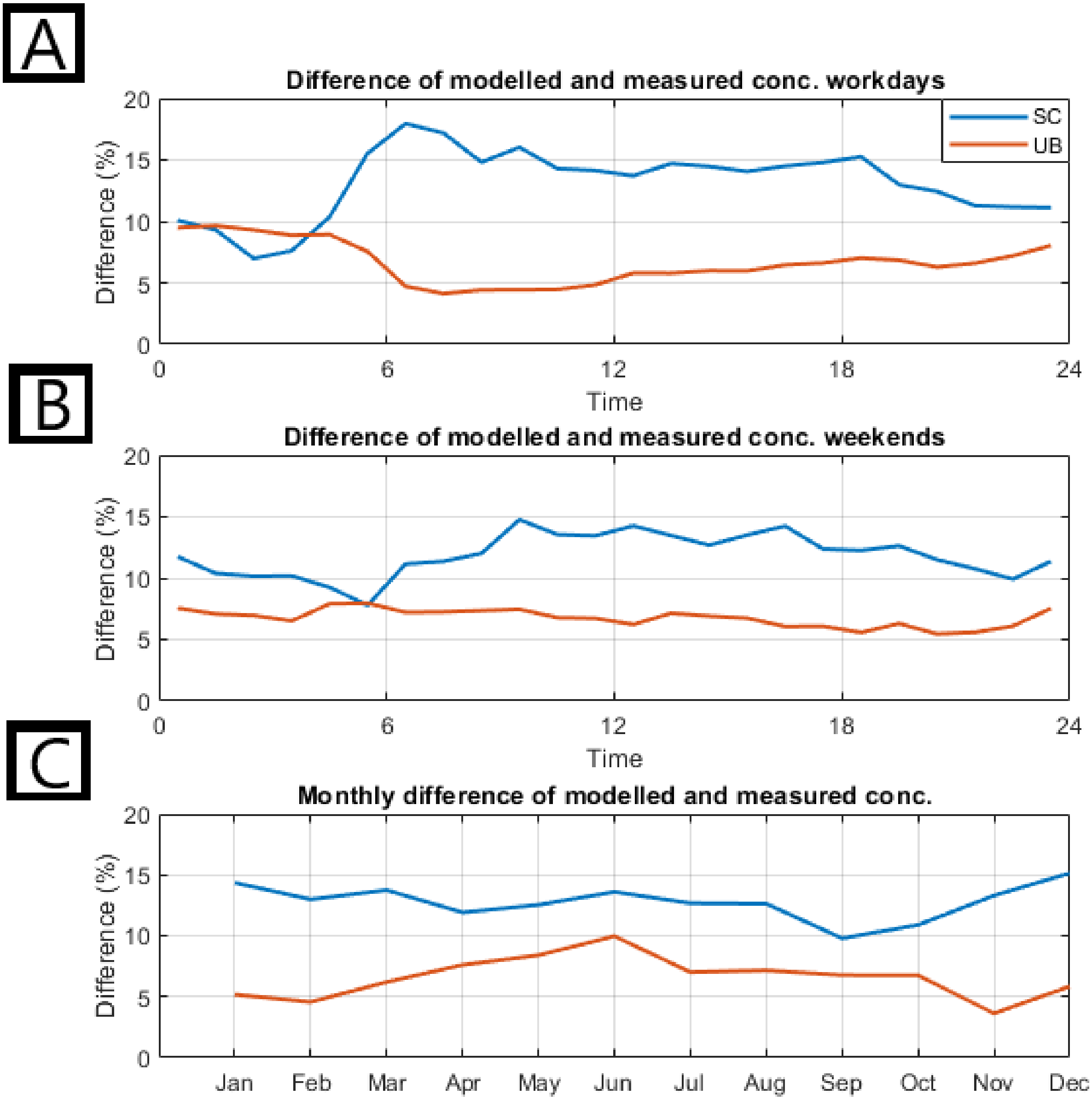

Figure S11: Average differences between modelled and measured concentrations for workdays (A), weekends (B) and months (C)at SC and UB.

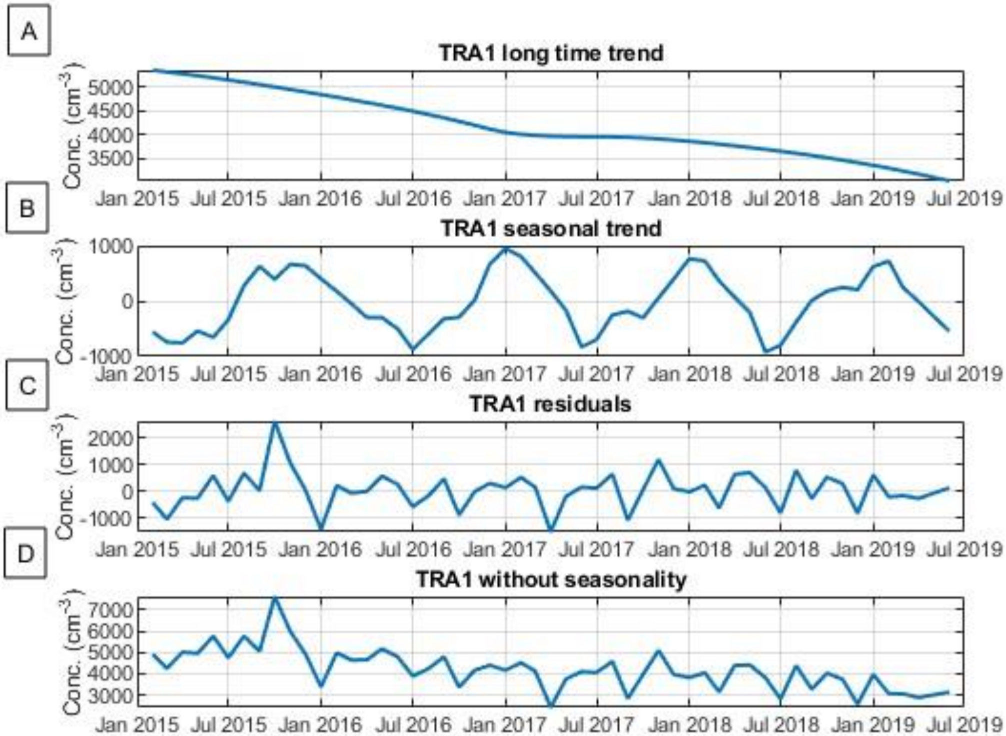

Figure S12: Decomposition of TRA1 factor time series into a long-time trend (A), seasonal trend (B), and residuals using Seasonal Trend Decomposition Procedure Based on Loess (Cleveland, et al., 1990) (C). D shows the LRT factor time series with the seasonality removed.

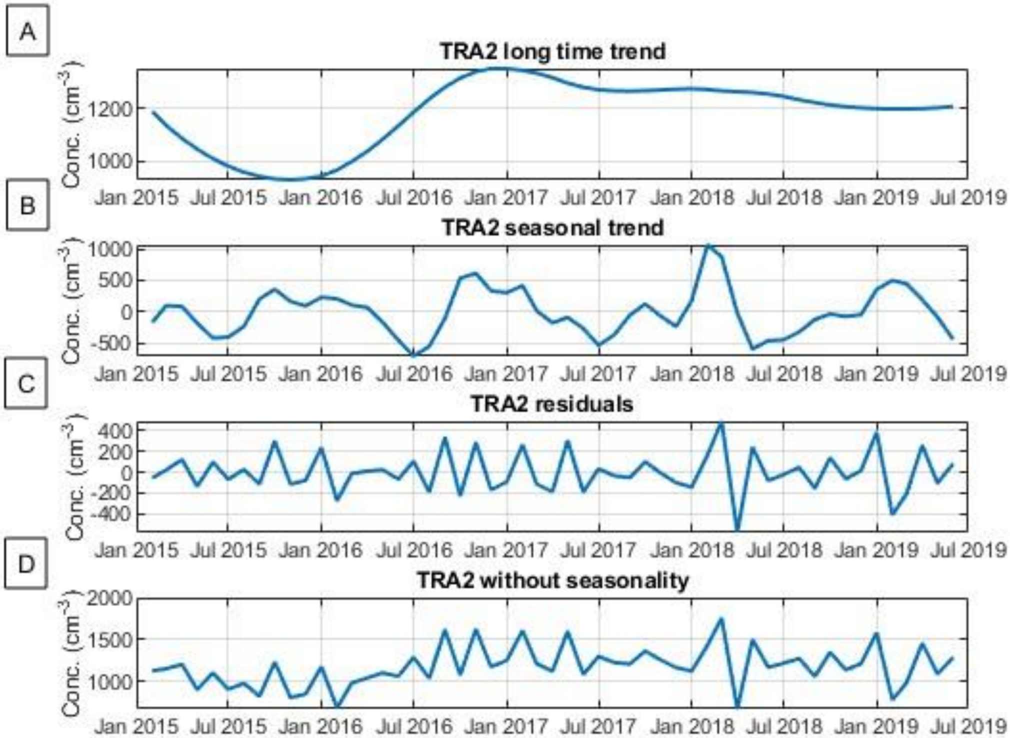

Figure S13: Decomposition of TRA2 factor time series into a long-time trend (A), seasonal trend (B), and residuals using SeasonalTrend Decomposition Procedure Based on Loess (Cleveland, et al., 1990) (C). D shows the LRT factor time series with the seasonality removed.

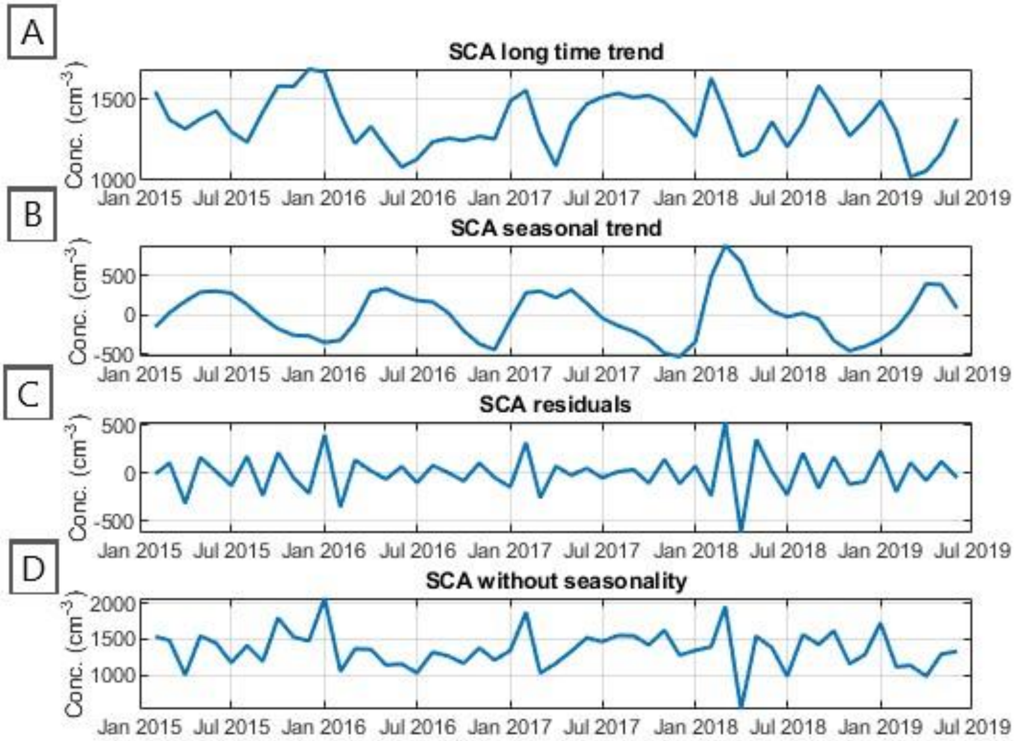

Figure S14: Decomposition of SCA factor time series into a long-time trend (A), seasonal trend (B), and residuals using SeasonalTrend Decomposition Procedure Based on Loess (Cleveland, et al., 1990) (C). D shows the LRT factor time series with the seasonality removed.

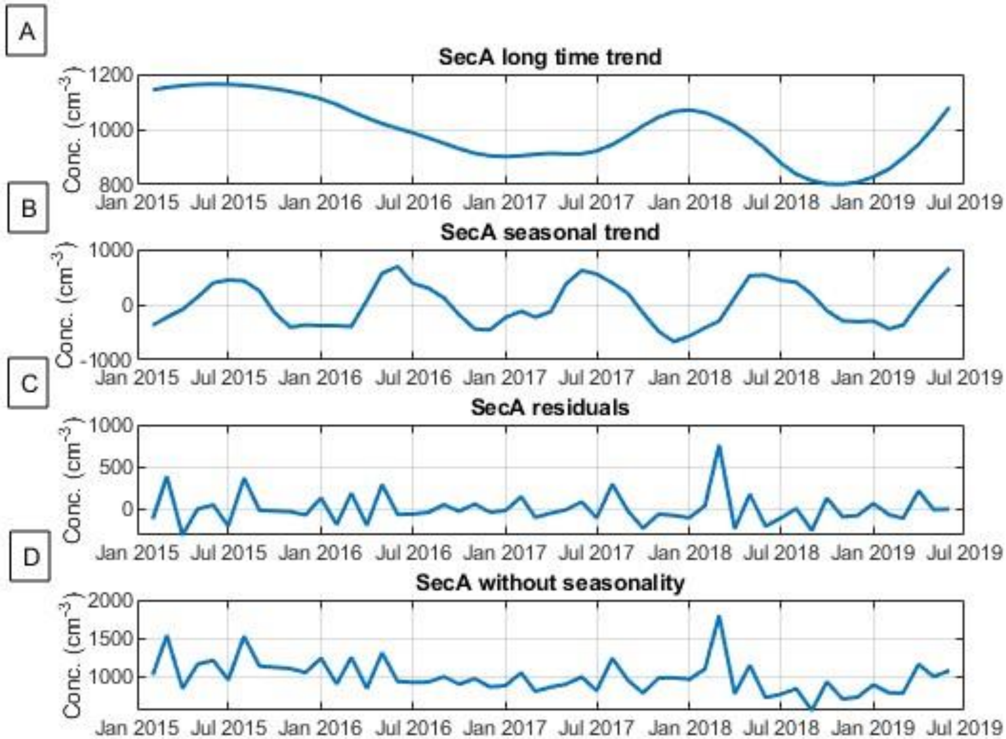

Figure S15: Decomposition of SecA factor time series into a long-time trend (A), seasonal trend (B), and residuals using Seasonal Trend Decomposition Procedure Based on Loess (Cleveland, et al., 1990) (C). D shows the LRT factor time series with the seasonality removed.

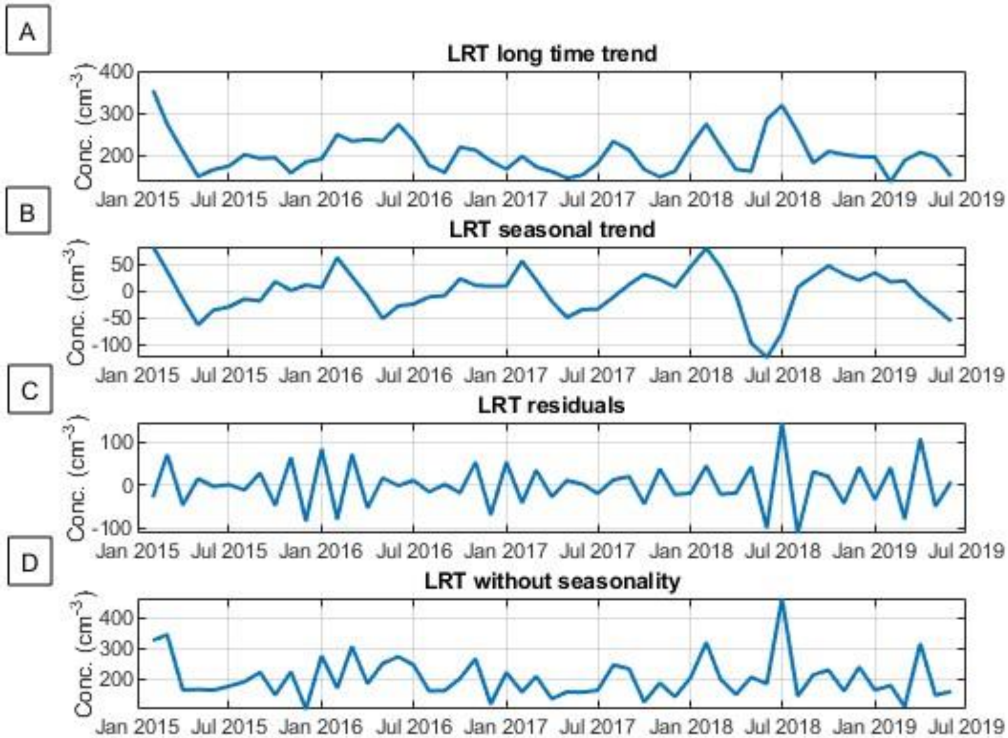

Figure S16: Decomposition of LRT factor time series into a long-time trend (A), seasonal trend (B), and residuals using Seasonal Trend Decomposition Procedure Based on Loess (Cleveland, et al., 1990) (C). D shows the LRT factor time series with the seasonality removed.

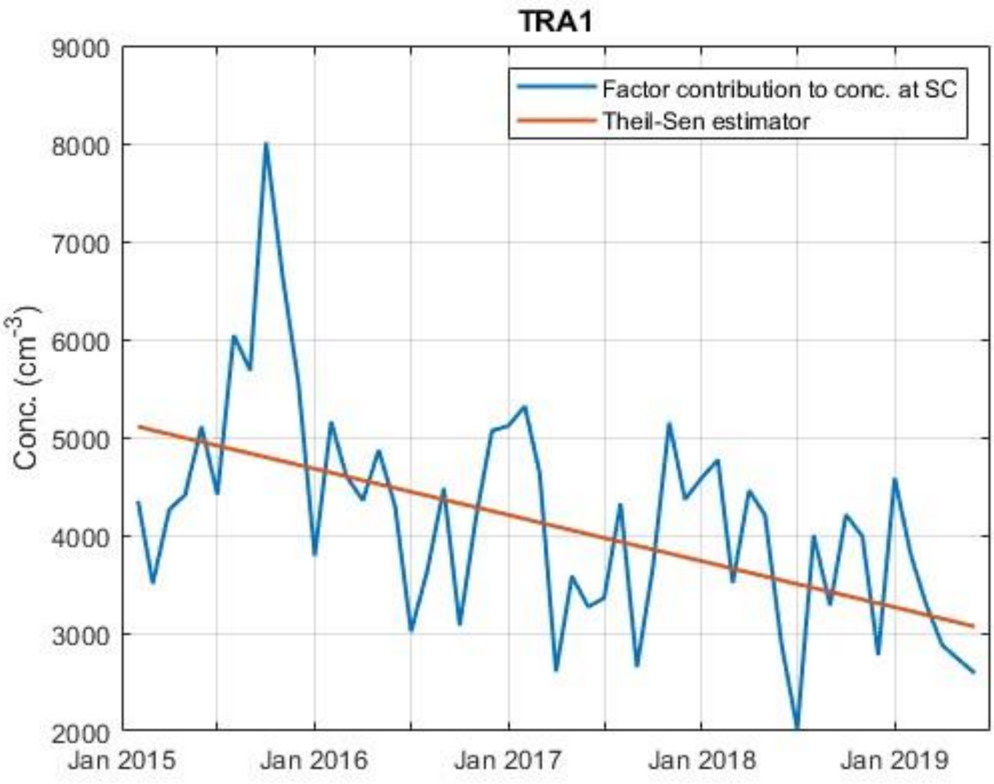

Figure S17: TRA1 factor time series and the fitted Theil-Sen estimator.

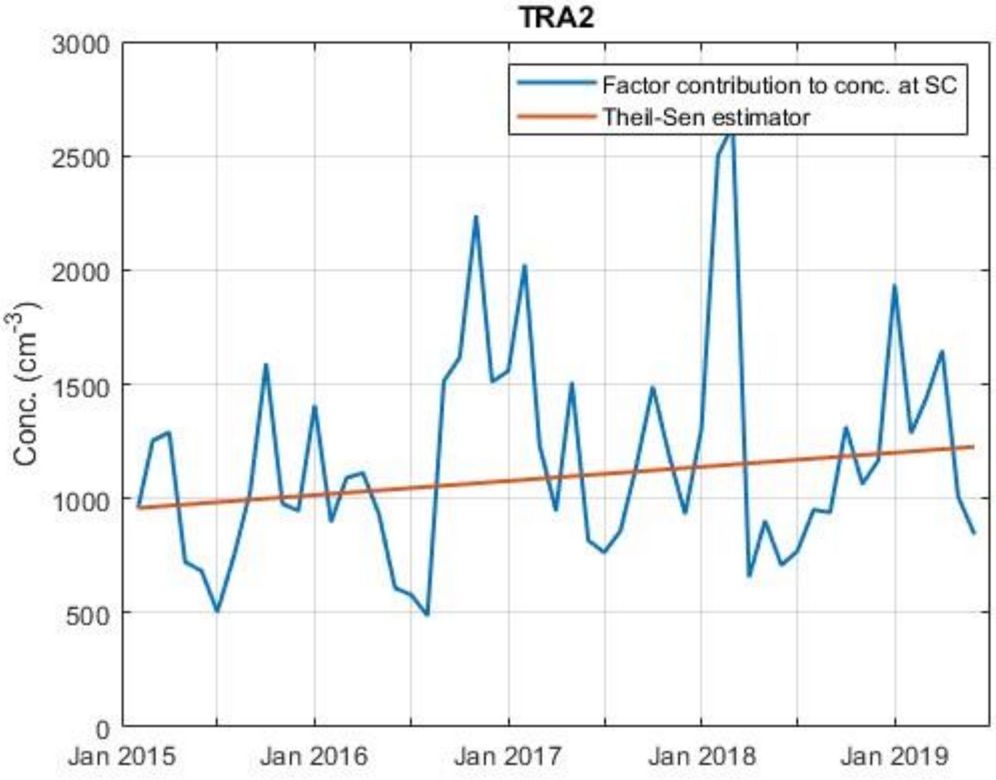

Figure S18: TRA2 factor time series and the fitted Theil-Sen estimator.

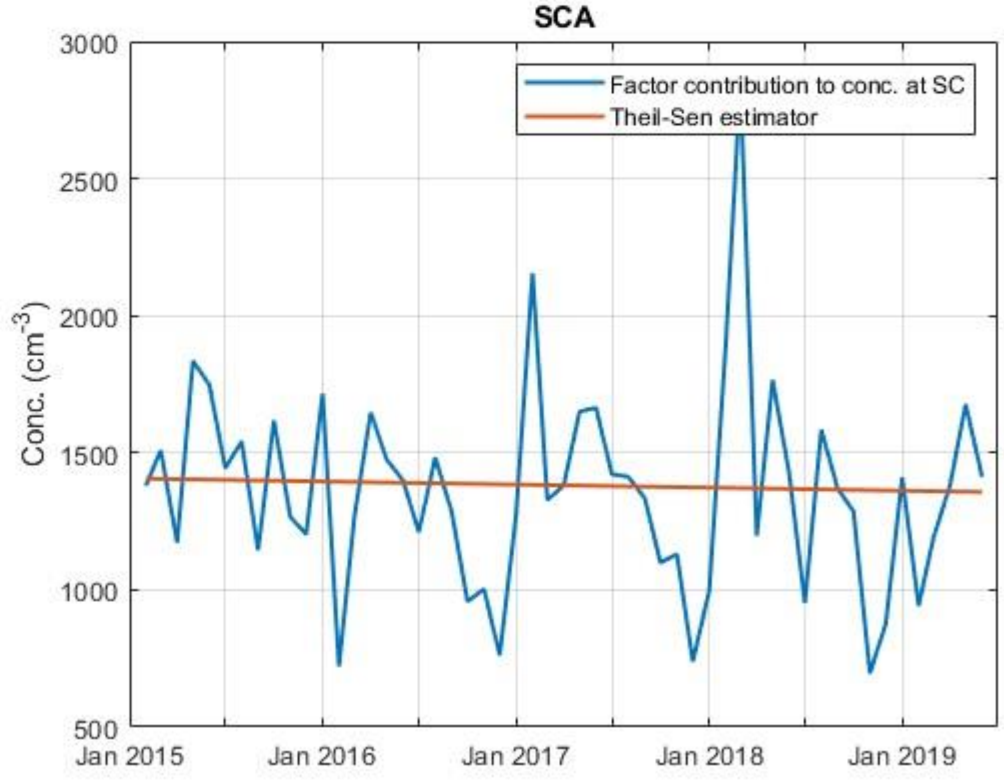

Figure S19: SCA factor time series and the fitted Theil-Sen estimator.

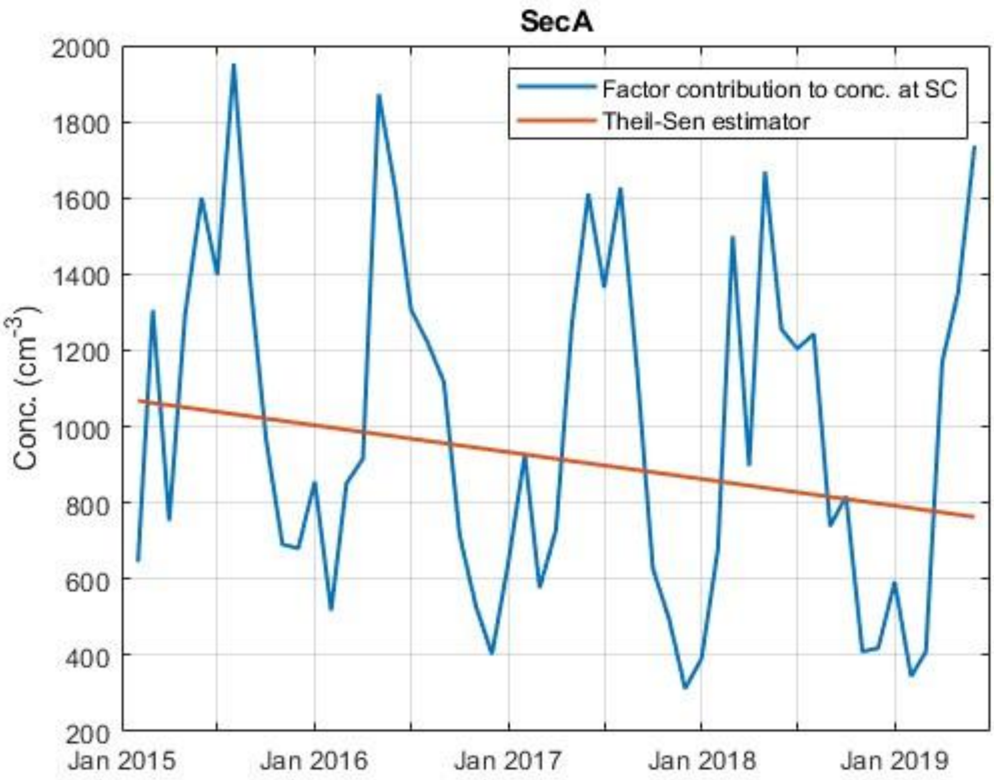

Figure S20: SecA factor time series and the fitted Theil-Sen estimator.

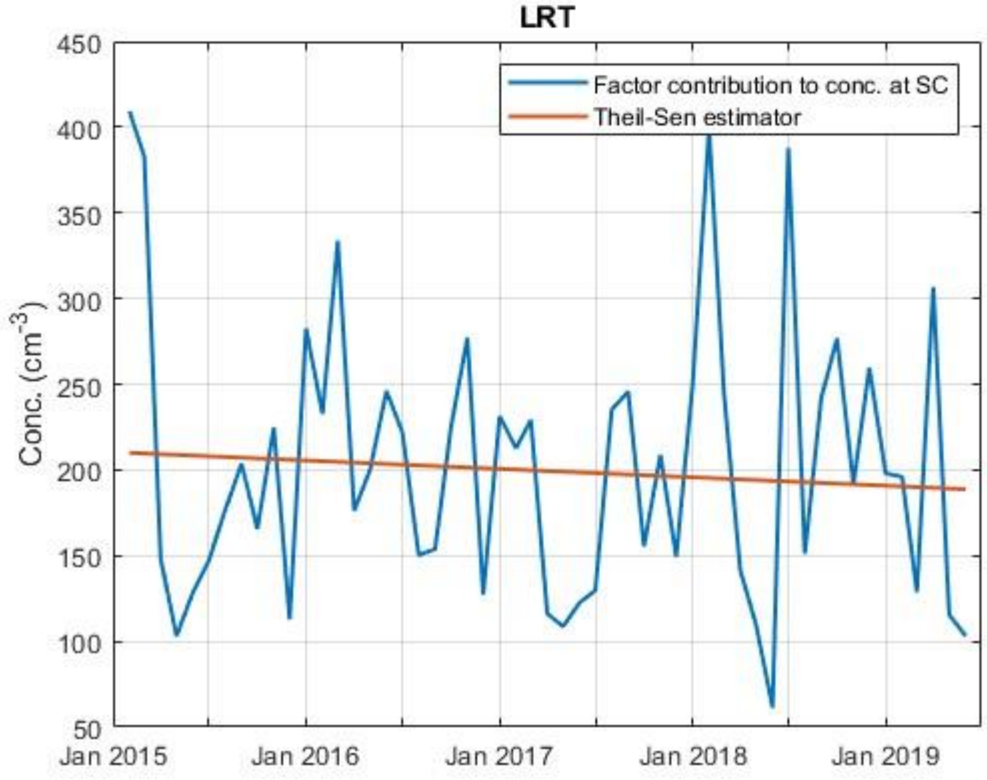

Figure S21: LRT factor time series and the fitted Theil-Sen estimator.

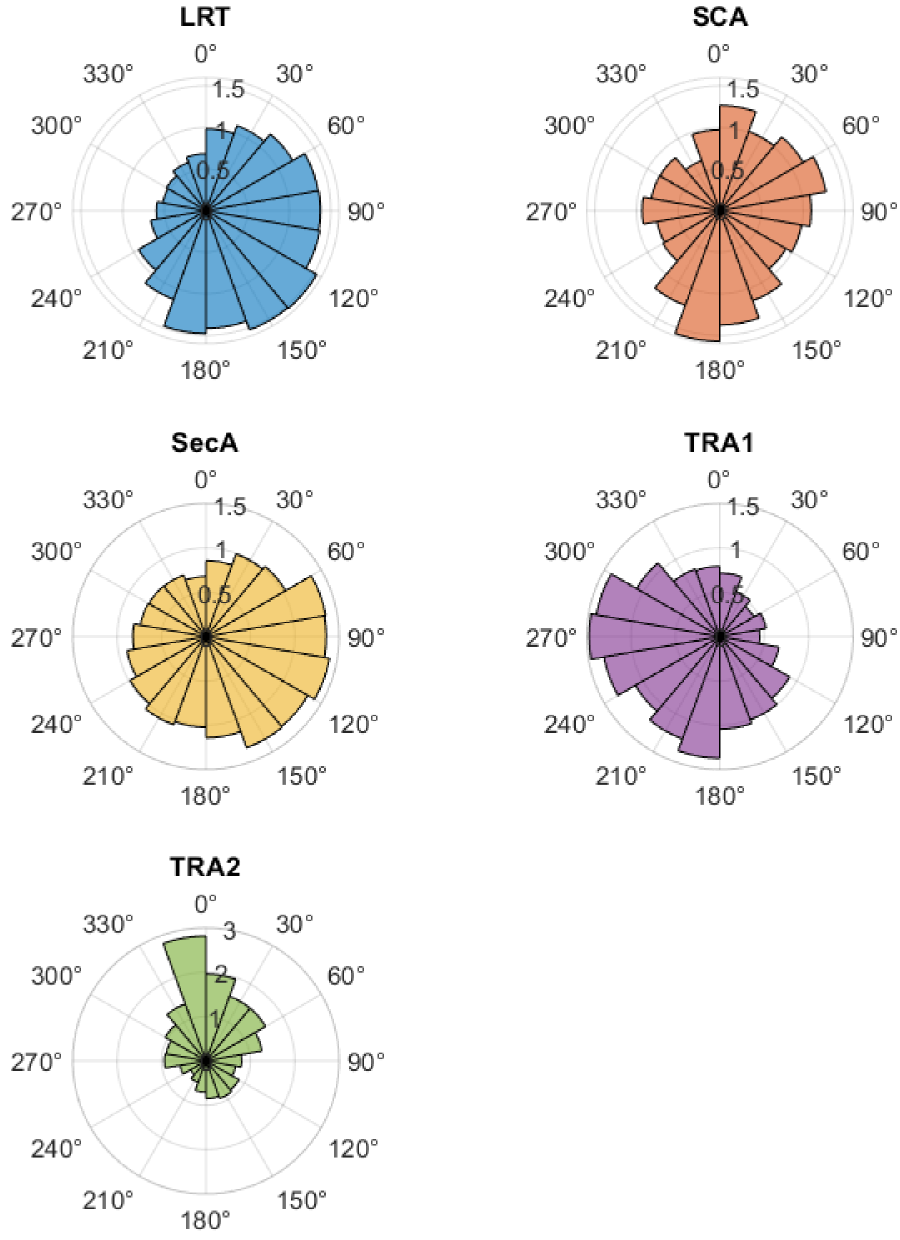

Figure S22: Scaled contributions of LRT, SCA, SecA, TRA1 and TRA2 factors from different wind directions.

References

Cleveland, R. B., Cleveland, W. S., & Terpenning, I.: STL: A seasonal-trend decomposition procedure based on loess. J. Off. Stat., 6(1), 3., 1990.